High transmission through a 90° bend in a polarization-independent single-mode photonic crystal waveguide

Adem Enes Erol* **and H. Sami Sözüer**
Physics Department, Izmir Institute of Technology, 35430 Izmir, Turkey
*ademerol@iyte.edu.tr

Abstract: We propose a polarization-independent single-mode waveguide, using a two-dimensional square photonic crystal with a complete band gap. The waveguide is tuned such that both TE and TM modes have the same group velocity and zero group velocity dispersion at the centergap frequency. We also present results for a 90° bend with transmission values of 98% for both modes.

OCIS codes: (130.5296) Photonic crystal waveguides; (230.5298) Photonic crystals.

References and links

1. L.Vivien, S. Laval, B. Dumont, S. Lardenois, A. Koster, and E. Cassan, "Polarization-independent single-mode rib waveguides on silicon-on-insulator for telecommunication wavelengths," Opt. Commun. **210**(1), 43–49 (2002).
2. S. P. Chan, C. E. Png, S. T. Lim, G. T. Reed, and V. Passaro, "Single-mode and polarization-independent silicon-on-insulator waveguides with small cross section," IEEE J. Lightwave Technol. **23**(6), 2103 (2005).
3. S. T. Lim, C. E. Png, E. A. Ong, and Y. L. Ang, "Single mode, polarization-independent submicron silicon waveguides based on geometrical adjustments," Opt. Express **15**(18), 11061–11072 (2007).
4. M. M. Milošević, P. S. Matavulj, B. D. Timotijević, G. T. Reed, and G. Z. Mashanovich, "Design rules for single-mode and polarization-independent silicon-on-insulator rib waveguides using stress engineering," IEEE J. Lightwave Technol. **26**(13), 1840–1846 (2008).
5. M. K. Chin, C. Xu, and W. Huang, "Theoretical approach to a polarization-insensitive single-mode microring resonator," Opt. Express **12**(14), 3245–3250 (2004).
6. E. Cassan, L. Vivien, and S. Laval, "Polarization-independent 90-turns in single-mode micro-waveguides on silicon-on-insula-tor wafers for telecommunication wavelengths," Opt. Commun. **235**(1), 83–88 (2004).
7. Y. Vlasov and S. McNab, "Losses in single-mode silicon-on-insulator strip waveguides and bends," Opt. Express **12**(8), 1622–1631 (2004).
8. A. Mekis, J. C. Chen, I. Kurland, S. Fan, P. R. Villeneuve, and J. D. Joannopoulos, "High transmission through sharp bends in photonic crystal waveguides," Phys. Rev. Lett. **77**(18), 3787 (1996).
9. A. Mekis, S. Fan, and J. D. Joannopoulos, "Bound states in photonic crystal waveguides and waveguide bends," Phys. Rev. B **58**(8), 4809 (1998).
10. H. S. Sözüer and H. D. Şengün, "Photonic crystal assisted 90 waveguide bend," Int. J. Mod. Phys. B **25**(16), 2167–2182 (2011).
11. K. Y. Lee, C. C. Tsai, T. C. Weng, Y. L. Kuo, C. W. Kao, K. Y. Chen, and Y. J. Lin, "Transmission characteristics of 90 bent photonic crystal waveguides," Fiber Integrated Opt. **25**(1), 29–40 (2006).
12. E. Lidorikis, M. L. Povinelli, S. G. Johnson, and J. D. Joannopoulos, "Polarization-independent linear waveguides in 3D photonic crystals," Phys. Rev. B **91**(2), 19 (2003).
13. A. Cicek and B. Ulug, "Polarization-independent waveguiding with annular photonic crystals," Opt. Express **17**(20), 18381–18386 (2009).
14. H. Wu, D. S. Citrin, L. Jiang, and X. Li, "Polarization-independent single-mode waveguiding with honeycomb photonic crystals," IEEE Photonics Technol. Lett. **27**(8), 840–843 (2015).
15. S. G. Johnson and J.D. Joannopoulos, "Block-iterative frequency-domain methods for Maxwell's equations in a planewave basis," Opt. Express **8**(3), 173–190 (2001).
16. A. Taflove and S. C. Hagness, *Computational Electrodynamics* (Artech House, 2005).

#253041 Received 4 Nov 2015; revised 7 Dec 2015; accepted 7 Dec 2015; published 10 Dec 2015

17. A. F. Oskooi, D. Roundy, M. Ibanescu, P. Bermel, J. D. Joannopoulos, and S. G. Johnson, "MEEP: A flexible free-software package for electromagnetic simulations by the FDTD method," Comput. Phys. Comm. **181**, 687–702 (2010).

1. Introduction

Single-mode and polarization-independence are desirable conditions for optical waveguides [1–6]. Single-mode operation is necessary to avoid signal distortion due to different mode group velocities. Even with single-mode operation, waveguide dispersion is another source of signal distortion, as the different frequency components of the signal traveling at different velocities would, given enough time, lead to signal corruption. In addition, polarization-independence is also necessary to avoid additional devices required for polarization management.

Single-mode and polarization-independent waveguides have been reported for silicon-on-insulator (SOI) rib waveguides [1, 2] and with rib waveguides having sidewall angles [4]. Single-mode and polarization-independent propagation based on SOI rib waveguides and photonic wires has been investigated at the submicron scale [3]. It has also been shown that a ridge waveguide, with critical width and etch depth, can be made to be polarization-independent and single-mode [5].

Waveguide bends are key elements for optical circuit applications. Hence, single-mode operation and polarization-independence are also critically important design considerations for waveguide bends. It has been shown that efficient polarization-independent 90°-turns can be achieved for single-mode SOI rib waveguides with corner mirrors and strip waveguides using bends with sufficiently large curvature radii [6], although surface roughness can severely increase bending losses [7]. Using two-dimensional (2D) photonic crystal (PhC) waveguides, highly efficient transmission of light around 90° bends has been demonstrated for transverse magnetic (TM) modes [8, 9]. Transmission of 90° bends, but only for transverse electric (TE) modes in a 2D setting, has been studied [10, 11]. High polarization-independent bend transmission has been demonstrated by a 3D structure consisting of two PhC slab waveguides with one waveguide stacked on top of the other [12], with each slab carrying a different polarization. Polarization-independent waveguiding and transmission through a 90° bend have also been demonstrated in 2D, although guidance is multimode and bend losses are high [13]. Recently, single-mode polarization-independent waveguiding in 2D PhC slabs has been demonstrated, but without a calculation of bending loss [14]. To our knowledge, present work is the first time high transmission through a bend is reported for a polarization-independent *and* single-mode 2D PhC waveguide.

2. Polarization-independent single-mode PhC waveguide

Our aim is to design a polarization-independent single-mode waveguide ideally with zero dispersion, and a 90° bend with the same properties. To do that, we first need to find a photonic crystal with a complete band gap for both polarizations to keep the signal from leaking at the bend. Since the bending angle is 90°, the most promising lattice is the square lattice in 2D. Thus our first task is to find the right photonic crystal geometry.

2.1. Choosing the photonic crystal

We first try circular Si rods in air. In the square lattice, there is no complete bandgap for dielectric Si rods in air. With air rods in a Si background, there is a small complete bandgap, about 4%, when the air rod radius is around $0.48a$, where a is the lattice constant. However, the Si walls between the air rods become too thin making these structures quite fragile.

#253041 Received 4 Nov 2015; revised 7 Dec 2015; accepted 7 Dec 2015; published 10 Dec 2015

Next we try annular dielectric rods in air. These structures possess a complete bandgap between the seventh and eighth bands. To maximize the band gap, we performed a two dimensional parameter search to find the optimal values for the outer and the inner radii, R_1 and R_2 respectively, of the annular rods with $\varepsilon = 13$ in air background. We calculated the lowest band gap for a total of 1223 different structures using block-iterative frequency-domain methods for Maxwell's equations in a planewave basis [15]. We find that the largest gap is 6.53% with $R_1 = 0.39a$ and $R_2 = 0.24a$. The results are displayed in Fig. 1(a). The complete photonic band

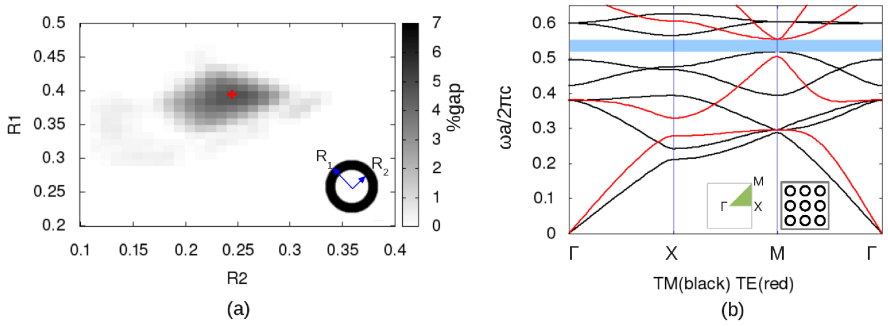

Fig. 1. (a) The gap-midgap ratio between the seventh and eighth bands versus the outer (R_1) and the inner (R_2) radii of the annular rod (inset) for a square lattice of dielectric rods with $\varepsilon = 13$ in air. The largest gap obtained with $R_1 = 0.39a$ and $R_2 = 0.24a$ is indicated by the red cross. (b) The corresponding band diagram. The complete photonic band gap of 6.53% is shaded blue. The center inset shows the irreducible Brillouin zone (shaded green).

gap lies in the range $0.5184 < \omega a/2\pi c < 0.5533$, where $\omega a/2\pi c$ is the normalized frequency. The centergap frequency is about $0.5359(2\pi c/a)$. The band diagram of this structure is shown in Fig. 1(b). These results are consistent with those of Cicek *et al* [13].

2.2. The design of the waveguide

Having found the optimal parameters of the photonic crystal, we now proceed with the design of the waveguide. We first consider a simple line defect waveguide formed by removing one row of annular rods. We model this structure using a supercell with size $15a \times a$ as shown in Fig. 2(a). The dispersion relation is displayed in Fig. 2(b) for the line defect waveguide. The line defect creates single guided TE and TM modes inside the complete photonic band gap (dashed curves). The normalized group velocity $|d\omega/d(ck)|$ of these guided modes as a function of the normalized frequency is displayed in Fig. 2(c) (dashed curves). This simple approach has two shortcomings. First, the group velocities of the two polarizations are not equal at the centergap frequency. Moreover, the group velocity dispersion is nonzero for each polarization. We aim to rectify these shortcomings by modifying the waveguide such that the group velocities will be equal at the centergap frequency for both modes, and, in addition, the dispersion would be ideally zero at the centergap frequency, again for both modes.

One approach used to achieve polarization-independent light guiding is to tailor the line defect such that the guided bands for the two polarizations overlap with the zero dispersion region at the center of the band gap. However this approach results in multimode waveguides [12, 13], with the extra modes having different group velocities.

Our approach is to tune the line defect by modifying the positions and the radii of two annular rods neighboring the line defect on both sides, as shown in Fig. 2(a). We again perform a fine grid search for the parameters r_1, r_2, and d in the range $r_1 : [0.37a, 0.45a]$, $r_2 : [0.18a, 0.35a]$, and $d : [0.95a, 1.05a]$ in steps of $0.01a$. We find that the optimal parameter set $r_1 = 0.41a$,

#253041 Received 4 Nov 2015; revised 7 Dec 2015; accepted 7 Dec 2015; published 10 Dec 2015

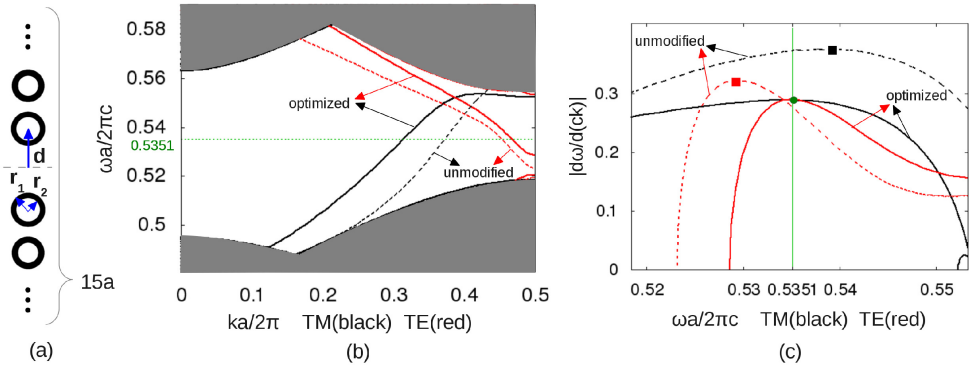

Fig. 2. (a)The supercell size of $15a \times a$ and the optimization parameters. (b)The dispersion relation for the unmodified line defect waveguide (dashed curves) and for the optimized line defect waveguide (solid curves). (c)The normalized group velocity versus the normalized frequency for the guided TE and TM modes of the unmodified line defect waveguide (dashed curves) and the optimized line defect waveguide (solid curves) with the optimal parameter set $r_1 = 0.41a$, $r_2 = 0.28a$ and $d = 0.97a$. The green filled circle is zero group velocity dispersion point with the same group velocity for each polarization.

$r_2 = 0.28a$ and $d = 0.97a$ makes group velocities of both TE and TM modes equal ($0.29c$) in Fig. 2(c) (green filled circle) at the frequency $0.5351(2\pi c/a)$ which is nearly at the centergap frequency. In addition, the group velocities have a local maximum with zero dispersion at the same frequency. Having the centergap frequency as the operating frequency is important for two reasons. One is that, at the centergap frequency, the mode profile of the guided wave will be highly localized at the line defect. Furthermore, since the photonic crystal cladding thickness is necessarily finite, the bending loss would be minimal as the penetration length into the photonic crystal will be minimal at the centergap frequency, thus minimizing "tunneling" losses through the cladding.

The normalized group velocities of the guided TE and TM modes are displayed in Fig. 2(c) (solid curves). For the optimal parameter set, the dispersion relations are also shown in Fig. 2(b) (solid curves). This modification does not introduce any extra guided modes. The optimized line defect waveguide is still single-mode for both polarizations.

3. The design of the 90° bend

To design the 90° bend with a low bending loss, one needs to resort to time-domain calculations. We use the finite-difference time-domain (FDTD) method [16] using a freely available software package [17]. The resolution is taken to be 64 points per unit cell size a. We use a simulation region of $68a \times 68a$ and the bend is located at a distance of $36a$ from the mode sources with a Gaussian profile in frequency. Flux-monitors are located just after the mode source for incident pulses and at a distance of $36a$ from the bend for transmitted pulses. The transmission of the bend is defined as the percent ratio of the output flux to the input flux. The input flux is computed from a separate simulation with a simulation region of $68a \times 45a$ on a straightened waveguide without the bend for the same total time.

We first try the simplest possible solution labeled corner-0 shown in Fig. 3(a), where two line defect waveguides meet abruptly at 90° with no "smooth" transition in between. For this simplest corner element we find that, at the operating frequency $0.5351(2\pi c/a)$, the transmission values for the TE and TM modes are 99.4% and 36.2%, respectively. While the transmission for the TE mode is excellent, the TM mode fares rather poorly. Since our aim is to design a

#253041 Received 4 Nov 2015; revised 7 Dec 2015; accepted 7 Dec 2015; published 10 Dec 2015

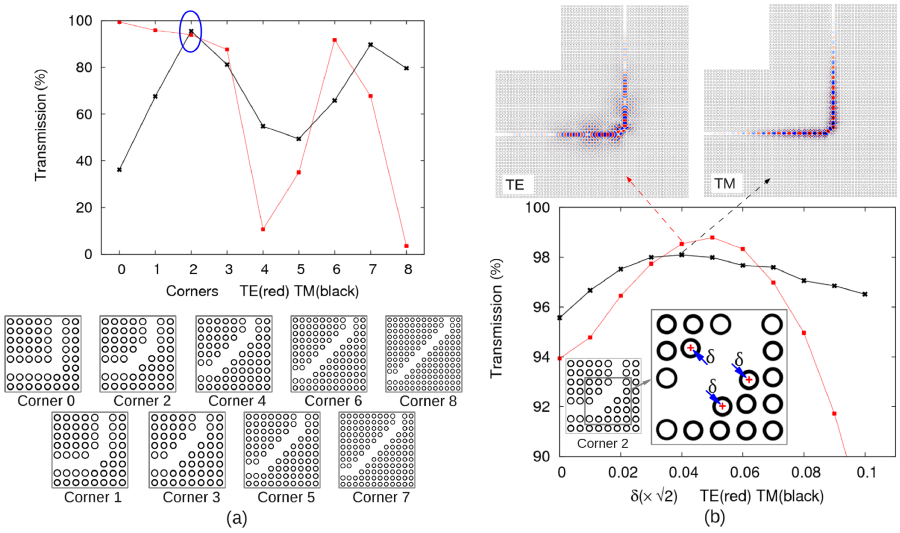

Fig. 3. (a)Transmission values for eight different diagonal corner elements, each of length $(n+1)\sqrt{2}a$, where n is the corner label. (b)Transmission through the corner element (inset) as a function of the parameter δ. The Gaussian packets passing through the bend at $\omega a/2\pi c = 0.5351$ with width $\Delta(\frac{\omega a}{2\pi c}) = 0.02$.

corner element with high transmission for both modes, we insert a diagonal element in between the two arms. We calculate the transmission values for different lengths of the diagonal element to determine the optimal length. We find that the transmission values fluctuate with the length of the diagonal element. This is understandable, since there would be reflections at the two 45° turns and the two reflections interfere constructively or destructively depending on the length of the diagonal element. The transmission maxima and the minima for each mode occur at slightly different lengths due to the different wave number, and hence different "effective wavelength" $2\pi/k$, for each mode at the operating frequency. This is analogous to the familiar interference of light through a thin film. The total transmission for both modes is maximum for corner-2, with 93.9% for TE, and 95.6% for TM.

To further fine-tune the corner element to maximize the transmission, we try slightly shifting the annular rods, whose centers are indicated by red crosses in Fig. 3(b). A shift of about $0.057a$ increases the transmission values by several percent to 98.5% for TE, and 98.1% for TM.

To understand the high transmission more clearly in addition to constructive and destructive interference explanation, we investigate the diagonal element as a short waveguide which is modeled using a supercell in Fig. 4(a). The dispersion relation for the diagonal element is shown in Fig. 4(b). At the operating frequency $0.5351(2\pi c/a)$, there are one TM and two TE localized guided modes as shown in the inset of Fig. 4(b). The normalized group velocities of the modes of the diagonal element are displayed in Fig. 4(c). The TM mode has nearly zero dispersion at the operating frequency, while the two TE modes have nonzero dispersion. This results in a slight widening of the Gaussian wave packet for the TE mode, while the TM mode passes through with little or no dispersion, as can be seen in Fig. 5(b).

Figure 5(a) shows the transmission through the bend as a function of the normalized frequency. Transmission is greater than 90% for both polarizations in the range between $w = 0.531$ and $w = 0.538$. High transmission ($\geq 95\%$) is achieved in the range $0.5323 < \omega a/2\pi c < 0.5373$ (shaded gray) for each polarization. The normalized group velocities for the straight waveguide are also shown in Fig. 5(a). In this range (shaded gray), the straight waveguide has similar group

#253041 Received 4 Nov 2015; revised 7 Dec 2015; accepted 7 Dec 2015; published 10 Dec 2015

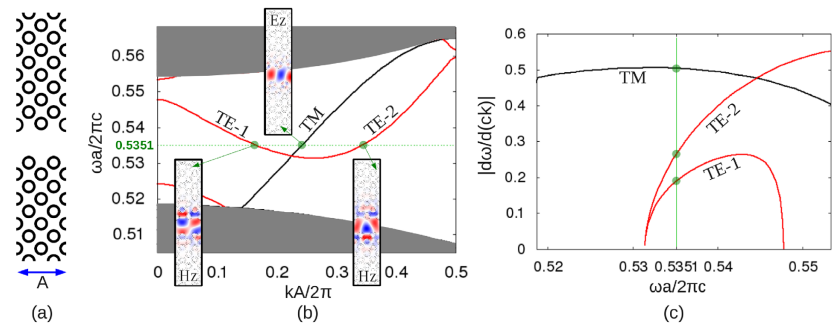

Fig. 4. (a) The supercell size of $10\sqrt{2}a \times A$ where $A = 2\sqrt{2}a$. (b)The dispersion relation for the diagonal element and modal profiles (inset) of TM, TE-1 and TE-2 modes at the normalized frequency $\omega a/2\pi c = 0.5351$. (c)The normalized group velocity of the TE and TM modes as a function of the normalized frequency.

velocities and nearly-zero dispersion for each polarization. We obtain the highest transmission of 98.6% (98.1%) at $\omega a/2\pi c = 0.5343$ (0.5351) for TE (TM) mode. The FDTD simulations of a Gaussian packet before and after passing through the corner element are displayed in Fig. 5(b).

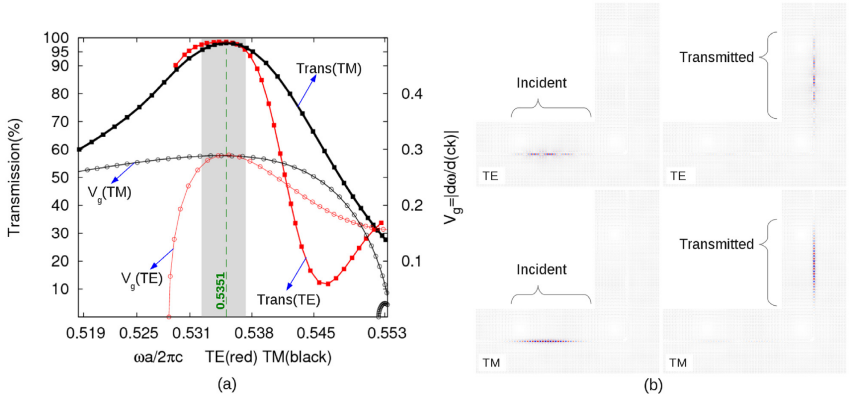

Fig. 5. (a)Transmission through the bend as a function of the normalized frequency in the range $0.5184 < \omega a/2\pi c < 0.5533$. The range $0.5323 < \omega a/2\pi c < 0.5373$ is shown as shaded gray. Also shown are the group velocity curves of the straight waveguide. (b) Incident pulses and transmitted pulses for TE and TM modes.

4. Conclusion

Using a two-dimensional square lattice of annular dielectric rods, we have demonstrated a polarization-independent single-mode waveguiding system which has the same group velocity and zero group velocity dispersion at the centergap frequency $0.5351(2\pi c/a)$. We find that the transmission through the bend is greater than 98% for both polarizations at this frequency. In the range $0.5323 < \omega a/2\pi c < 0.5373$ transmission values of more than 95% are obtained for both modes and the straight waveguide has close group velocities and nearly-zero dispersion for each polarization. Our future work will include 3D calculations for structures presented here, it is necessary for a realistic design that also addresses the vertical confinement issue.

#253041 Received 4 Nov 2015; revised 7 Dec 2015; accepted 7 Dec 2015; published 10 Dec 2015